Electrolyte Effects on the Chiral Induction and on Its Temperature Dependence in a Chiral Nematic Lyotropic Liquid Crystal

Ute C. Dawin,[†,§] Mikhail A. Osipov,[‡,#] and Frank Giesselmann*[,†]

Institute of Physical Chemistry, Universität Stuttgart, Pfaffenwaldring 55, D-70569 Stuttgart, Germany, and Department of Mathematics, University of Strathclyde, Livingstone Tower, 26 Richmond Street, Glasgow G1 1XH, United Kingdom

Received: March 21, 2010; Revised Manuscript Received: May 14, 2010

We present a study on the effect of added CsCl and of temperature variation on the chiral induction in a chiral nematic lyotropic liquid crystal (LC) composed of the surfactant cesium perfluorooctanoate (CsPFO), water, and the chiral dopant D-Leucine (D-Leu). The chiral induction was measured as the helical pitch *P*. The role of the additives CsCl and D-Leu on the phase behavior is investigated and discussed. The thermal stabilization effect of CsCl is shown to lead to an apparent salt effect on the pitch when the pitch is compared at a constant temperature. This apparent effect is removed by comparing the pitch measured for different salt concentrations at a temperature relative to the phase-transition temperatures; thus, the real salt effect on the pitch is described. High salt concentrations are shown to increase the pitch, that is, hinder the chiral induction. The effect is discussed in terms of a decreased solubilization of the amphiphilic chiral solute D-Leu in the micelles due to the salt-induced screening of the surfactant head groups and the consequential denser packing of the surfactants. The temperature variation of the pitch is investigated for all CsCl concentrations and is found to be essentially independent of the salt concentration. The temperature variation is analyzed and discussed in the context of a theoretical model taking into account specific properties of lyotropic liquid crystals. A hyperbolic decrease of the pitch is found with increasing temperature, which is known, from thermotropic liquid crystals, to stem from pretransitional critical fluctuations close to the lamellar phase. However, the experimental data confirmed the theoretical prediction that, at high temperature, that is, far away from the transition into the lamellar phase, the pitch is characterized by a linear temperature dependence which is determined by a combination of steric and dispersion chiral interactions. The parameters of the theoretical expression for the pitch have been determined by fitting the experimental data. The analysis of the salt concentration dependence of these parameters indicates that the chiral induction mechanism of D-Leu is dominated by chiral steric interactions.

Introduction

The liquid crystalline (LC) state of matter is characterized by long-range order of anisometric building blocks in at least one dimension. Depending on the nature of the building blocks, two liquid crystalline classes are defined. In thermotropic liquid crystals (TLCs), the building blocks are, in most cases, large organic molecules of anisometric shape, and the LC state is controlled mainly by temperature. In contrast, lyotropic LCs (LLCs) occur in aqueous solutions of amphiphilic (surfactant) molecules in a certain range of both temperature and amphiphile concentration. The building blocks of LLCs are anisometric aggregates of 100 and more amphiphiles. Different LC phases are distinguished according to the type of long-range order and structure. In the nematic (N) phase, the building blocks exhibit long-range orientational order, that is, the principal axes of the building blocks are, on average, aligned along a common axis specified by the so-called director **n**. This is shown in Figure 1a for a nematic LLC phase with disk-like amphiphile ag-

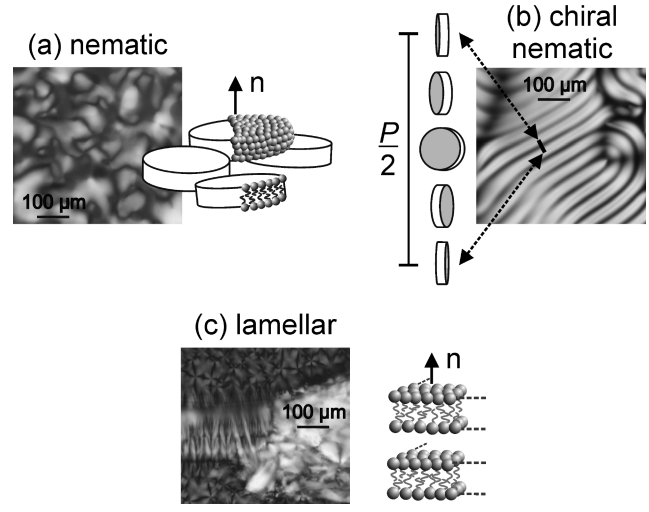

Figure 1. (a) Schlieren texture and model of the nematic (N) LLC host phase from CsPFO and water with disk-like micelles. (b) Fingerprint texture and model of the chiral nematic (N*) phase; the micelles represent the helical modulation of the director **n** with the pitch *P* induced by doping the host phase with 0.59 mol % D-Leu. (c) Typical texture of a lamellar phase (chiral L_α* or nonchiral L_α) as found by cooling the sample in (b). Model of the local layer structure of the lamellar phase with alternating surfactant double layers and water layers (water not drawn).

* To whom correspondence should be addressed. Fax: +49 711 685 62569. Tel: +49 711 685 64460. E-mail: f.giesselmann@ipc.uni-stuttgart.de.
† Universität Stuttgart.
‡ University of Strathclyde.
§ E-mail: u.dawin@ipc.uni-stuttgart.de.
# E-mail: mao@maths.strath.ac.uk. Fax: +44 141 548 3345. Tel: +44 141 548 3655.

10.1021/jp102547p
Published on Web 07/23/2010

gregates (micelles) which occur in the nematic LLC phase of CsPFO (see ref 1 and references therein).

At lower temperature and/or higher amphiphile concentration, compared to the N phase, a phase with layer structure can occur, which is termed the lamellar (L_α) phase for LLCs and the smectic-A (SmA) phase for TLCs. The building blocks in both isosymmetric phases show long-range orientational order and one-dimensional positional order. The layer normal is parallel to the director. In the L_α phase, the amphiphiles are packed into infinitely elongated flat double layers with a thickness of about double the surfactant molecule length and with the polar molecular heads pointing toward the water that spaces the lamellae (see Figure 1c). In the SmA phase, the layers are usually monolayers, depending on the chemical constitution of the phase-building molecules.

When chirality is introduced into a nematic phase (TLC or LLC), for example, by adding a small amount of a chiral solute (dopant), the chiral nematic (N*) phase is observed, which is also known as the cholesteric phase for historic reasons. The structure of the N* phase manifests chirality on a macroscopic level due to the presence of the helical superstructure of the director field; this is shown schematically in Figure 1b where single disk-like micelles represent the local director orientation. The helical periodicity (pitch) P is often in the micrometer range, and the helix can be directly observed in the polarizing optical microscope as a periodic stripe pattern ("fingerprint texture") with the period $P/2$. In the chiral lamellar (L_α*) or chiral smectic-A (SmA*) phase, a helical superstructure does not exist, and the pitch is not defined.

In lyotropic and thermotropic N* phases, the pitch is known to depend mainly on the chemical nature of the dopant and its concentration. For low dopant concentrations, that is, below 5 mol % in many cases, the inverse pitch increases linearly with the dopant concentration. The slope of this linear part characterizes the chiral induction power, that is, the helical twisting power (HTP), of a dopant.[2] The pitch is also influenced by the nature of the nematic host phase, although to a smaller extent, and by the temperature.

The temperature dependence of the pitch in thermotropic N* phases generally describes a decreasing hyperbolic function with increasing temperature (see, for example, refs 3−5). (We neglect here the phenomenon of helix sense inversion, which manifests itself in an additional strong pitch−temperature variation since in LLCs, this phenomenon is, to our knowledge, only known in chiral nematic LLC phases from polymers but not in those from classic ionic surfactants.) Close to the transition into the smectic-A phase, the pitch increases strongly due to pretransitional critical fluctuations and an increase of the twist elastic constant of the phase (see the Theoretical Basis section). At higher temperature, the pitch is approximately constant with T or decreases slightly in a linear way. In LLCs, however, two different pitch−temperature behaviors $P(T)$ have been found at temperatures far from the pretransitional fluctuations, (A) P increases linearly with decreasing T and (B) P increases strongly close to the nematic−lamellar transition T(N*L_α*) in the same way as described above for thermotropic LCs.[6,7] Theoretical considerations, which are sketched in the Theoretical Basis section, have related these two $P(T)$ behaviors to different mechanisms of the chiral induction. In case (A), the chiral induction is based on dispersive chiral interaction between dopants in adjacent micelles. In case (B), the chiral induction is dominated by steric chiral interaction between distorted micelles, the distortion arising from chiral steric dopant−amphiphile interactions (see refs 8−10 and the Theoretical Basis section). The molecular mechanisms controlling the chiral induction power have been under discussion for more than 20 years (see ref 11 and references therein). In a very recent study, the dopant location and dopant dynamics have been investigated via a spin resonance technique, and the reduced dopant dynamics has been proposed as a determining factor for strong chiral induction power in the LLC system investigated there.[11]

The chiral induction in lyotropic LCs is potentially influenced by further parameters such as added electrolytes. Especially in LLCs from ionic amphiphiles, pronounced salt effects on the phase behavior have been found in numerous studies (see ref 1 and references therein). Adding salt, even at very low concentrations, to a nematic LLC can shift the temperature range of the LC state to substantially higher temperatures (shift of about 10 K at 1 mol % salt).[1] With increasing salt concentration, the nematic phase is destabilized in favor of the lamellar phase, and at sufficiently high concentration, phase separation occurs. One may assume that the salt added to an N* phase can influence not only the phase behavior but also the chiral induction via, for example, screening of dispersion interactions, variation of the charge distribution at the micellar surface, or change of micellar size and anisotropy. Due to the diversity of possible electrolyte−pitch interactions, a theoretical treatment has not been established yet, but a few experimental studies have addressed the issue. Goozner et al. added NH_4Cl to an N* phase of decylammonium chloride (DACl) in water doped with the chiral amphiphile octane-(2*S*)-aminium chloride and found a linear decrease of the pitch with added salt.[12] In contrast, Ocak et al. reported a parabolic increase of P upon the addition of salt to a selection of different N* phases. One of these differs from Goozner's system only regarding the chiral dopant since Ocak also used a DACl/water host phase and NH_4Cl as an added salt but L-mandelic acid as the chiral dopant.[13]

The strong difference between the results obtained by Goozner and Ocak stimulated us to analyze in more detail the experimental conditions applied in both cases. Most interestingly, in both studies, the pitch measurements were performed at constant temperature, ignoring two temperature-dependent phenomena (i) the temperature dependence of the pitch and (ii) the salt effect on the phase behavior. In fact, a salt-induced temperature shift of both the N* phase boundaries and the pitch−temperature behavior results in an apparent change of the pitch if the latter is compared for the same temperature. This phenomenon is demonstrated in Figure 2 for both $P(T)$ behaviors described above.

Figure 2a shows the case for the $P(T)$ behavior (A). We assume that the $P(T)$ curve is shifted to higher temperatures proportionally to the concentration of added salt and that the $P(T)$ behavior remains essentially unchanged. The inset in Figure 2a shows how, under these conditions, a comparison of P at a chosen constant temperature T_x results in a linear decrease of the pitch. When applying the same procedure and assumptions to the hyperbolic $P(T)$ behavior (B), the pitch measured at T_x increases parabolically with increasing electrolyte concentration (see Figure 2b). Case (a) fits exactly to the results described by Goozner et al., who also reported the linear $P(T)$ behavior for their system. Unfortunately, the salt effect on the phase behavior was not considered in their study. Case (b) reflects very well the observations reported by Ocak et al., who also found the appearance of the lamellar phase when adding salt, which confirms our assumption of the salt effect on the phase behavior. However, Ocak et al. do not describe the $P(T)$ behavior in their systems, and our considerations remain hypothetical in this case. Nevertheless, our analysis of the experimental conditions in both

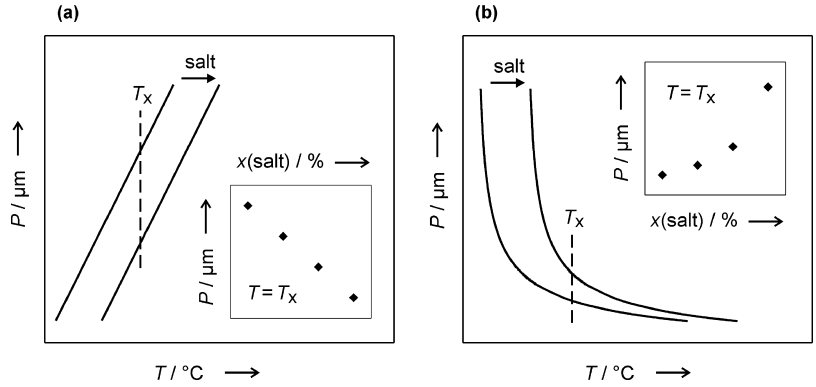

Figure 2. Illustration of the occurrence of an apparent salt effect on the pitch if the latter is compared for the same temperature. (a, b) Idealized cases for both $P(T)$ behaviors (A) and (B), respectively. See text for details. All axes are scaled linearly.

SCHEME 1: Molecular Structures of the Surfactant Cesium Pentadecafluorooctanoate (CsPFO) and the Chiral Dopant D-Leucine (D-Leu) in Both Forms, the Zwitterionic Form Dominating at the Isoelectric pH Value and the Protonated Cationic Form Dominating at Lower pH Values

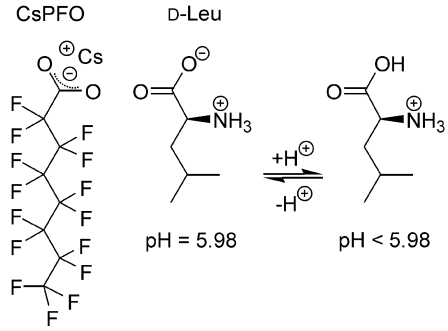

studies suggests strongly that the $P(T)$ behavior and the salt effect on the phase behavior have to be taken into account in order to reveal the real electrolyte effect on the chiral induction. This can be achieved by choosing a temperature relative to one of the transition temperatures for the comparison of the pitch values.

In this paper, we present a systematic investigation of the salt effects on a chiral nematic LLC host phase. Our aim is to separate the real salt influence on the chiral induction (measured as the helical pitch of the N* phase) from the apparent salt effect on the pitch resulting from the interplay between the electrolyte-induced change of the phase behavior and the temperature dependence of the pitch. For the achiral nematic LLC host phase, we chose a well-known phase formed by the simple ionic surfactant cesium pentadecafluorooctanoate (CsPFO) in water at the CsPFO/water mass ratio of 55/45. As chiral dopant D-Leucine (D-Leu) was added at a concentration of 0.59 mol % (see Scheme 1 for molecular structures).

The system exhibits, with increasing temperature, the phase sequence lamellar−chiral nematic−isotropic. CsCl was added at concentrations between 0.16 and 2.54 mol % with respect to the pseudoternary system CsPFO/water/CsCl. For each CsCl concentration, we investigated both the phase behavior and, where appropriate, the pitch−temperature behavior. With increasing salt concentration, the transition temperatures were substantially elevated, and the nematic phase was destabilized. However, compared to the ternary system CsPFO/water/CsCl with the same concentrations, the extent of the salt influence on the phase behavior was smaller in the presence of D-Leu. This phenomenon can be explained via the increased micellar curvature due to the solubilization of the small leucine molecule at the micellar surface. The pitch in the quarternary N* phase of CsPFO/water/D-Leu/CsCl was found to diverge close to the transition into the lamellar phase, which is an indication for chiral induction mechanism (B). However, we revealed that an additional linear term according to induction mechanism (A) is required to fit the experimental data correctly. This combination of both induction mechanisms is not surprising since the mechanisms described as (A) and (B) are extreme cases of the same theoretically derived function (see eq 13 in the Theoretical Basis section). The added CsCl did not change the general shape of the $P(T)$ curve. This is readily visible by superimposing the $P(T)$ behavior of all CsCl concentrations using the transition temperature $T(N^*L_\alpha^*)$ as a reference point. Therefore, in first order, there is no salt effect on the chiral induction. However, superimposing the $P(T)$ curves by choosing the clearing point $T(N^*I)$ as a reference temperature revealed a small remaining salt effect on the pitch. With increasing CsCl concentration, the pitch at $T(N^*-I)$ was slightly elevated, that is, the chiral induction was hindered by the added salt. The effect is discussed in terms of the reduced solubilization of the dopant molecule in the micelle due to the salt-induced screening of the surfactant head groups and the subsequent denser packing of the surfactants.

Theoretical Basis

In this section, we aim at providing a concise description of the theoretical background on which the data analysis and fitting of the pitch−temperature behavior (see the Results and Discussion section) are based.

Close to the transition from the chiral nematic phase into the smectic-A/lamellar phase, small regions with positional smectic-like order of the building blocks appear. This short-range smectic order is characterized by the coherence length $\xi = \xi_0(T - T_c)^{-\nu}$, which diverges toward the apparent critical temperature T_c. In the case of a second−order N*−SmA* transition, the critical temperature is the transition temperature, while in the case of the first-order transition, T_c is the lower absolute stability limit of the chiral nematic phase, that is, $T_c < T(N^*SmA^*)$ in the case of the first-order transition.

The critical exponent ν is typically between 0.5 and 0.7 (see, for example, refs 3−5). This pretransitional behavior manifests itself in an anomalous increase of the twist and bend elastic constants K_{22} and K_{33}, respectively, and hence of the cholesteric pitch $P = K_{22}/\lambda$. Here, λ is the chiral material parameter (mathematically a pseudoscalar) in the expression for the distortion free energy for pure twist deformation

$$F_{\text{twist}} = \frac{1}{2}K_{22}(\mathbf{n}\cdot\text{curl }\mathbf{n})^2 + \lambda(\mathbf{n}\cdot\text{curl }\mathbf{n}) \quad (1)$$

where $\mathbf{n}$ is the director. The pseudoscalar quantity λ vanishes for a nonchiral system and possesses opposite signs for opposite enantiomers.

In contrast to K_{22}, which diverges at the second-order cholesteric smectic-A transition and increases strongly close to the first-order transition, the chiral parameter λ remains finite, and hence, in this range, the helical pitch P has qualitatively the same temperature variation as the twist elastic constant K_{22}. As a result, in the vicinity of the transition into the smectic-A phase, the pitch can be expressed as

$$P = P_0 + \kappa'(T - T_c)^{-\nu} = P_0 + \kappa(T/T_c - 1)^{-\nu} \quad (2)$$

where ν is the critical exponent for the coherence length, P_0 is the pitch in the absence of smectic ordering, and κ depends on the twist elastic constant of the nematic phase.[14,15] These results are general and can be applied to both thermotropic and lyotropic cholesteric liquid crystals.

One notes, however, that eq 2 describes the temperature variation of the helical pitch only close to the transition into the smectic-A phase. Away from the transition, the temperature variation is determined by other factors, including, in particular, the so-called excluded volume effects.[16] The molecular theory of cholesteric ordering, which takes into account excluded volume effects, has been developed by several authors.[17−20] Here, we briefly summarize the main results of these studies which are relevant to the present work.

In the mean-field-like approximation, the free energy of the cholesteric (or inhomogeneous nematic) state can be written in the form

$$F = \rho k_B T \int f(\mathbf{a}\cdot\mathbf{n}(\mathbf{r}))\ln f(\mathbf{a}\cdot\mathbf{n}(\mathbf{r}))\,d\mathbf{a}\,d\mathbf{r} + \frac{1}{2}\rho^2\int V_{\text{eff}}(\mathbf{a}_1,\mathbf{r}_{12},\mathbf{a}_2)f(\mathbf{a}_1\cdot\mathbf{n}(\mathbf{r}_1))f(\mathbf{a}_2\cdot\mathbf{n}(\mathbf{r}_2))\,d\mathbf{a}_1\,d\mathbf{a}_2\,d\mathbf{r}_1\,d\mathbf{r}_2 + \frac{1}{2}\rho^2 k_B T\int \Theta(r_{12} - \xi_{12})f(\mathbf{a}_1\cdot\mathbf{n}(\mathbf{r}_1))f(\mathbf{a}_2\cdot\mathbf{n}(\mathbf{r}_2))\,d\mathbf{a}_1\,d\mathbf{a}_2\,d\mathbf{r}_1\,d\mathbf{r}_2 \quad (3)$$

where the unit vectors $\mathbf{a}_1$ and $\mathbf{a}_2$ are in the direction of the primary axes of the molecules 1 and 2, respectively, ρ is the number density, $\mathbf{r}_{12}$ is the intermolecular vector and $f(\mathbf{a}_1\cdot\mathbf{n}(\mathbf{r}_1))$ is the orientational distribution function. $V_{\text{eff}}(\mathbf{a}_1, \mathbf{r}_{12}, \mathbf{a}_2)$ is the effective attraction interaction energy between the molecules 1 and 2 modulated by the molecular shape, and ξ_{12} is the closest distance of approach for two molecules with fixed relative orientation. $\Theta(r_{12} - \xi_{12})$ is a step function which describes the steric cutoff; $\Theta(r_{12} - \xi_{12}) = 0$ if the molecules penetrate each other (i.e., $r_{12} < \xi_{12}$), and $\Theta(r_{12} - \xi_{12}) = -1$ otherwise.

In eq 3, the first term is the orientational entropy, the second term represents the internal energy of the system, and the third term is the so-called packing entropy which depends only on the excluded volume for the two molecules. The free energy in eq 3 describes the inhomogeneous nematic state with the director distribution $\mathbf{n}(\mathbf{r})$. This free energy can be split into two parts which describe the free energy of the homogeneous nematic state and the distortion free energy (for pure twist deformation) given by eq 2. This can be achieved by performing the gradient expansion of the orientational distribution function $f(\mathbf{a}_2\cdot\mathbf{n}(\mathbf{r}_2))$

$$f(\mathbf{a}_2\cdot\mathbf{n}(\mathbf{r}_2)) = f(\mathbf{a}_2\cdot\mathbf{n}(\mathbf{r}_1)) + (\mathbf{r}_{12}\cdot\nabla)f(\mathbf{a}_2\cdot\mathbf{n}(\mathbf{r}_1)) + \frac{1}{2}(\mathbf{r}_{12}\cdot\nabla)^2 f(\mathbf{a}_2\cdot\mathbf{n}(\mathbf{r}_1)) + \ldots \quad (4)$$

Substitution of the expansion (eq 4) into the free energy (eq 3) enables one to obtain a general expression for the distortion free energy which depends on the gradients of the director. One notes that in eq 3, only the internal energy and the packing entropy contribute to the distortion free energy because the corresponding terms depend on the orientation of the director at two different points $\mathbf{r}_1$ and $\mathbf{r}_2$.

As shown in ref 21, after employing the gradient expansion, the chiral coefficient λ in the expression for the helical pitch can be expressed in the following general form

$$\lambda = \lambda_{\text{att}} + \lambda_s k_B T \quad (5)$$

where

$$\lambda_{\text{att}} = \frac{1}{2}\rho^2\int(\mathbf{C}_{\text{att}}\cdot(\mathbf{a}_1\times\mathbf{n}))(\mathbf{a}_1\cdot\mathbf{n})f(\mathbf{a}_1\cdot\mathbf{n})f'(\mathbf{a}_2\cdot\mathbf{n})\,d\mathbf{a}_1\,d\mathbf{a}_2 \quad (6)$$

and

$$\lambda_s = \frac{1}{2}\rho^2\int(\mathbf{C}_s\cdot(\mathbf{a}_1\times\mathbf{n}))(\mathbf{a}_1\cdot\mathbf{n})f(\mathbf{a}_1\cdot\mathbf{n})f'(\mathbf{a}_2\cdot\mathbf{n})\,d\mathbf{a}_1\,d\mathbf{a}_2 \quad (7)$$

where $f'(\mathbf{a}_2\cdot\mathbf{n})$ is the derivative of $f(\mathbf{a}_2\cdot\mathbf{n})$ with respect to $(\mathbf{a}_2\cdot\mathbf{n})$. Here, the vectors $\mathbf{C}_{\text{att}}$ and $\mathbf{C}_s$ are determined by the effective intermolecular attraction and repulsion, respectively

$$\mathbf{C}_{\text{att}} = \rho^2\int V_{\text{eff}}(\mathbf{a}_1,\mathbf{r}_{12},\mathbf{a}_2)\mathbf{r}_{12}\,dr_{12} \quad (8)$$

and

$$\mathbf{C}_s = \rho^2\int\Theta(r_{12} - \xi_{12})\mathbf{r}_{12}\,dr_{12} \quad (9)$$

Even without taking into account the details of chiral intermolecular interactions, one may conclude that the coefficient λ can be expressed as a sum of two terms as given by eq 5. The first term is determined by the chiral intermolecular attraction potential, while the second term is determined by the chirality of molecular shape. It is important to note also that the attraction contribution is approximately temperature-independent while the steric contribution is essentially proportional to temperature.

Both intermolecular attraction and repulsion contribute also to the elasticity coefficients of the nematic LC. It is possible to obtain a similar expression also for the twist elastic constant K_{22}, which can be written in the form

$$K_{22} = K_{\text{att}} + K_s k_B T \quad (10)$$

where K_{att} is determined by intermolecular attraction, K_s is determined by excluded volume effects, and k_B is the Boltzmann constant.[19,20] As a result, the pitch of the cholesteric helix (far

from the transition into the smectic phase) can be written in the following general form

$$P = 2\pi\frac{K_{att} + K_s k_B T}{\lambda_{att} + \lambda_s k_B T} \quad (11)$$

Equation 11 has been widely used to interpret the temperature variation of the helical pitch in lyotropic polymer LCs composed of helical rigid macromolecules,[16] including the explanation of the temperature-induced helix inversion, which may occur when the two terms in the denominator of eq 11 possess opposite signs.

A rough analysis of eq 11 enables one to correlate different types of experimentally observed temperature variations of the pitch (far from the transition temperature) and the different chiral induction mechanisms (A) and (B) described in the introduction for LLCs.[8−11] If the chiral induction mechanism is dominated by chiral dispersion interactions, (case (A)) the corresponding contribution λ_{att} is dominant over $\lambda_s k_B T$, and hence, a linear temperature dependence of the pitch is expected. In the case (B), when steric chiral interactions are predominant, the opposite inequality is valid, that is, $\lambda_{att} \ll \lambda_s k_B T$, and a hyperbolic temperature dependence of the pitch is observed, provided $K_{att} \gg K_s k_B T$, which is usually the case.

In the general case, eq 11 describes a nonlinear temperature variation of the pitch. However, within a restricted temperature interval, the pitch varies only slowly with temperature, and the function $P(T)$ can be expanded in powers of $T - T_0$ in the vicinity of some temperature T_0. Taking into account only the linear term, one obtains the following approximate expression for the pitch

$$P = 2\pi\frac{K_{att} + K_s k_B T_0}{\lambda_{att} + \lambda_s k_B T_0} + 2\pi\frac{k_B K_{att} K_s(\lambda_{att}/K_{att} - \lambda_s/K_s)}{(\lambda_{att} + \lambda_s k_B T_0)^2}(T - T_0) \quad (12)$$

One notes that according to eq 12, the rate of change of the helical pitch is proportional to the difference between dispersion and steric contributions to the pitch $\lambda_{att}/K_{att} - \lambda_s/K_s$. As discussed above, this equation is valid far from the transition into the smectic-A phase. In the vicinity of the transition, there exists an additional temperature-dependent contribution to the pitch, which is determined by smectic fluctuations and is given by eq 2. As a result, the temperature variation of the pitch is described by the following general equation, which combines all contributions (eqs 2 and 12) and which is expected to be valid in the whole temperature range of the cholesteric phase.

$$P = \kappa(T/T_c - 1)^{-\nu} + a + bT \quad (13)$$

where

$$a = 2\pi\frac{K_{att} + K_s k_B T_0}{\lambda_{att} + \lambda_s k_B T_0} - 2\pi T_0\frac{k_B K_{att} K_s(\lambda_{att}/K_{att} - \lambda_s/K_s)}{(\lambda_{att} + \lambda_s k_B T_0)^2}$$

$$b = 2\pi T\frac{k_B K_{att} K_s(\lambda_{att}/K_{att} - \lambda_s/K_s)}{(\lambda_{att} + \lambda_s k_B T_0)^2}$$

Empirical expressions of the form of eq 13 have been successfully used by several authors to fit the temperature variation of the pitch for a number of thermotropic chiral nematic liquid crystals (see, for example, refs 3−5).

According to the above considerations, the temperature variation of the pitch in a lyotropic N* phase can reveal important aspects of the character of the molecular interactions, that is, the chiral induction mechanism. We will use the findings in the analysis of the $P(T)$ behavior in the Results and Discussion section.

Experimental Section

Cesium perfluorooctanoate (CsPFO) was prepared as described previously.[1] D-Leucine (D-Leu) was purchased from Aldrich at a purity of at least 99% percent and an enantiomeric excess of 97%. Cesium chloride (CsCl) was purchased from Aldrich at 99.9% purity. Both additives were used without further purification. Two LLC stock solutions were prepared from (i) CsPFO and bidistilled water at the mass ration 55:45 and (ii) from CsPFO, bidistilled water, and D-Leu. In the ternary solution, the relative concentration of CsPFO and water was the same as in that (i), and the D-Leu concentration was 0.59 mol %. The solutions were homogenized by repeated shear mixing and tempering at 40 °C. To each stock solution, CsCl was added to obtain nonchiral samples with 0.17, 0.98, 1.69, and 2.49 mol % CsCl and chiral samples with 0.16, 1.20, 1.69, and 2.48 mol % CsCl, respectively. The error in CsCl concentration was less than ±2% for the lowest CsCl concentration and decreased down to less than ±0.5% for the highest CsCl concentration. The homogenized sample solutions were sucked into rectangular glass capillaries (Camlab Microslide) of about 5 cm length and with an inner thickness of either 200 μm for the nonchiral samples or 300 μm for the chiral samples to avoid helix suppression by confinement effects. The capillaries were flame-sealed.

Phase transitions were determined by temperature-dependent texture observations using an optical polarizing microscope (Leica DM LP) equipped with a hotstage (Instec TS 62). The absolute error in temperature was about ±0.1 °C. The phase diagrams presented in this work were recorded upon heating. For an accurate correlation of both phase transition temperatures and the helical pitch of the chiral nematic samples, a position in the middle of the capillary was chosen and kept during the whole measurement. All pitch measurements were performed upon cooling since the fingerprint texture developed more homogeneously upon cooling from the isotropic phase than upon heating from the lamellar phase. In the ternary CsPFO/water/D-Leu sample without CsCl, an analyzable homogeneous fingerprint texture could only be obtained by applying an external magnetic field. The capillary was placed in a permanent iron magnet with its width of 3 mm parallel to the homogeneous magnetic field of about 1.4 T. After several days at a few degrees below the N*−I transition, the sample had developed a relatively homogeneous fingerprint texture with the helix axis of the domains orientated mainly parallel to the magnetic field, that is, perpendicular to the light propagation direction. The sample was transferred to the preheated hotstage and measured immediately.

The pitch was obtained from images of the fingerprint texture. The images were recorded with a digital camera (Nikon Coolpix 990) mounted on the microscope and were analyzed using the image processing package ImageJ.[22] A two-dimensional fast Fourier transformation (2D-FFT) was performed which yields a diffraction-like pattern. The spacing of the intensity maxima

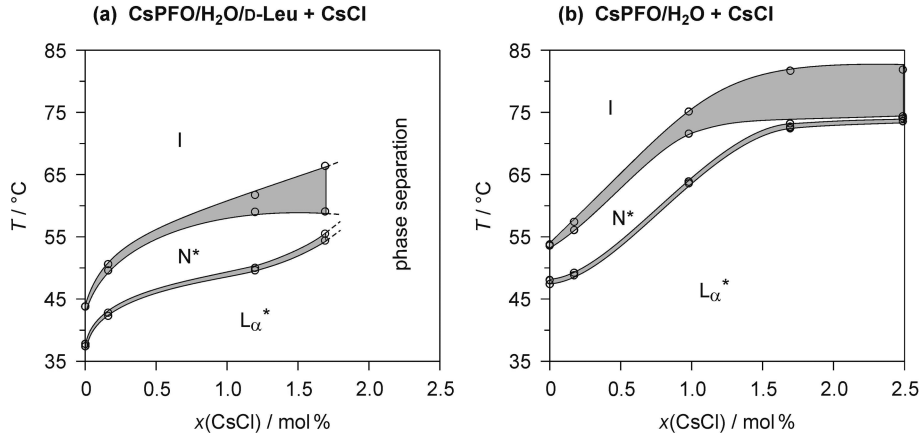

Figure 3. Pseudobinary phase diagrams for the addition of CsCl to (a) the chiral host phase containing 0.59 mol % D-Leu and to (b) the non-chiral CsPFO/water host phase (weight ratio of 55/54). The curves are guides to the eye. Two-phase regions are marked in gray.

in the diffraction pattern was correlated with the periodicity of the stripe pattern via calibration with an optical grid. The pitch was obtained as the double of the stripe periodicity according to the definition shown in Figure 1. The relative error of the pitch was about ±5%. The largest pitch values in the sample with 1.20 and 1.69 mol % CsCl could not be analyzed via the 2D-FFT method since too few fingerprint domains were present in the images. The pitch was obtained directly from the texture images using the distance measuring tool of the program Adobe Acrobat Professional (version 8.1.3) and a calibration.

The pH value of the ternary stock solution (with CsPFO/water/D-Leu) was measured using pH indicator strips (Merck) with a subdivision of 0.5 pH.

Results and Discussion

Effects of CsCl and D-Leu on the Phase Behavior. In Figure 3a, the effect of added CsCl on the phase behavior of the chiral nematic host phase CsPFO/water/D-Leu is presented as a pseudobinary phase diagram.

With increasing CsCl concentration, several effects appear. At low salt concentration, the LC state is generally stabilized. All transition temperatures are elevated by several Kelvin (5−10 K at 1.20 mol % CsCl), and the N* phase is broadened by a few Kelvin. Further increase of the CsCl concentration still increases the N*−L_α* transition temperature until it reaches a limit at around 1.5 mol % CsCl. Above this salt concentration, only the I−N* coexistence region continues to broaden, and the pure N* phase almost vanishes completely.

These salt effects are well-known and have been discussed in detail in ref 1 and references therein. In that work, also further salt effects were observed, namely, the disappearance of the N phase at a slightly increased CsCl concentration and a salting-out-like phase separation at moderate concentrations of the salts LiCl, NaCl, and KCl. These phenomena arise via multiple mechanisms. The most important of these shall be sketched briefly (see ref 1 for details).

(i) Added counterions screen the electrostatic repulsions between equally charged head groups both at the same micellar surface and between adjacent aggregate surfaces. Thereby, electrolytes increase the size and anisometry of the micelles and especially favor the formation of lamellae. According to the theoretical considerations by Boden et al., the enhancement of the micelle size and anisometry leads to a thermal stabilization of the nematic phase.[1,23]

(ii) The favoring of the lamellar phase at higher salt concentration can be illustrated by the packing parameter concept discussed in detail by, for example, Israelachvili.[1,24] According to the latter, lamellae are formed if the amphiphile head groups at the micellar surface are allowed to come close to each other (e.g., via screening of the electrostatic repulsions) so that the micellar curvature is almost zero.

(iii) The salting-out phenomenon arises on the one hand from dehydration of the phase by the added salt. On the other hand, the added salt increases intermicellar attractions which promote phase separation.

To reveal the effect of D-Leu for the phase behavior, the above results are compared with the effects of adding CsCl to the nonchiral phase from CsPFO and water. Figure 3b presents the respective pseudobinary phase diagram. The CsCl effects are qualitatively the same as those in the presence of D-Leu, but there are quantitative differences. Without D-Leu, the stabilizing salt effect is much more pronounced; for example, the transition temperatures are elevated by 10−20 K at 1.20 mol % CsCl. Obviously, the effects of D-Leu and CsCl on the phase behavior oppose each other, and D-Leu destabilizes the LLC state. The phenomenon can be accounted for by using the concepts (i) and (ii) described above for the effect of added salt. D-Leu is an amphiphile with a very short alkyl chain and can participate in the micelle formation. According to the packing parameter concept, small amphiphilic additives enhance the micelle curvature. This decreases the size and anisotropy of the aggregates and subsequently destabilizes the LLC state thermally and favors a micellar isotropic phase.[23] This process can even be enhanced if the head group of D-Leu is charged positively. The head group of D-Leu has a pH-dependent zwitterionic character (see Scheme 1). The pH of the ternary CsPFO/water/D-Leu stock solution was found to lie between 5.0 and 5.5, which is lower than the isoelectric point at pH = 5.98 for D-Leu.[25] Thus, the pH-dependent equilibrium given in Scheme 1 should be biased in our samples to the side where the D-Leu head group is positively charged.

In the sample with highest CsCl concentration (2.48 mol % with respect to the components CsPFO/water/CsCl), the presence of 0.59 mol % D-Leu (with respect to the components CsPFO/water/D-Leu) induces phase separation into an isotropic solution and a LLC phase with changed composition. The latter exhibits an L_α*−N* transition at around 75 °C, an N* phase of about 0.5 K width, and a clearing temperature of about 80 °C. A similar phase separation was also observed in a previous study in the ternary system components CsPFO/water/CsCl at a slightly increased CsCl concentration of 2.50 mol %.[1] Both

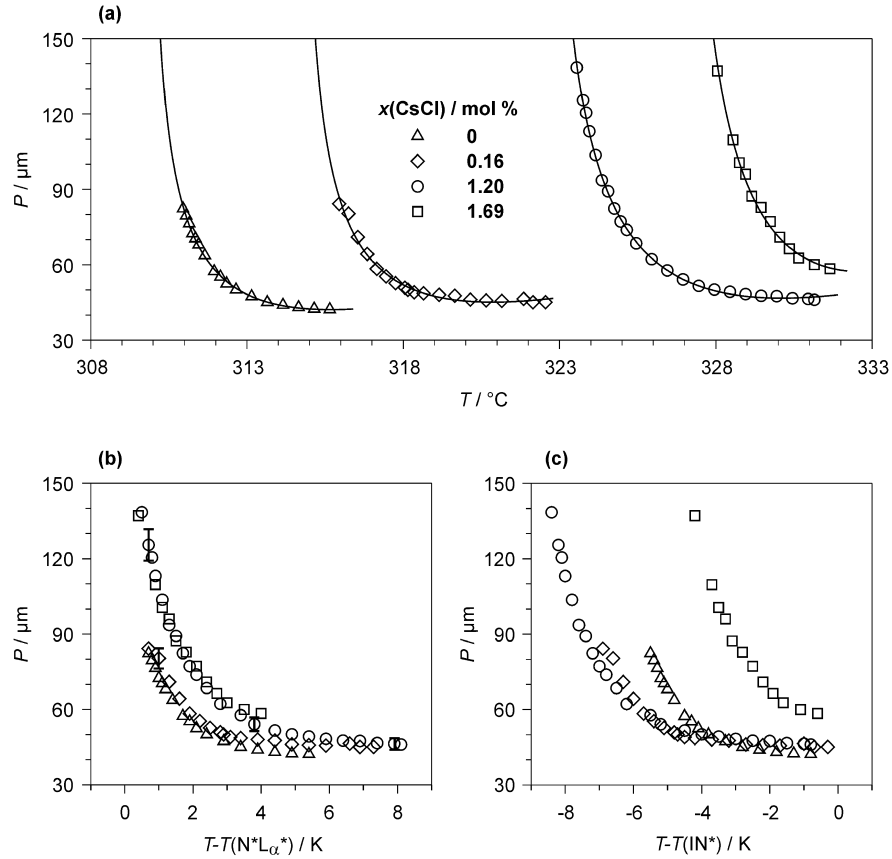

Figure 4. Pitch−temperature behavior for different CsCl concentrations plotted (a) against the temperature T, (b) against the relative temperature $T - T(L_\alpha{}^*N^*)$, and (c) against the relative temperature $T - T(IN^*)$. The solid lines in (a) are the best fits of eq 13 (see Table 1 and the text for details). The error bars for the pitch given in (b) are the same for all diagrams. The error of the temperature is included in the width of the data points.

TABLE 1: Best-Fit Parameter Values for Fitting the Experimental Pitch−Temperature Behavior to Equations 13 and 2[a] for the Fixed Exponent $\nu = 0.5$ and the Experimental Phase Transition Temperatures $T(N^*L_\alpha{}^*)$ Compared for the Different Salt Concentrations

					constant parameter		
x(CsCl)/mol %	κ/μm	$\nu^b/-$	$T_c{}^c$/K	$T(N^*L_\alpha{}^*)$/K	a/μm	$P_0{}^a/\mu$m	b/μm K^{-1}
0	6.56 ± 0.19	0.5	309.8	310.3	−1286 ± 115		4.06 ± 0.36
0.16	7.25 ± 0.43	0.5	314.7	315.3	−1351 ± 181		4.19 ± 0.56
1.20	14.29 ± 0.26	0.5	322.2	323.1	−2123 ± 101		6.30 ± 0.30
1.20[a]	9.81 ± 0.49	0.5	322.1	323.1		−20.9 ± 4.7	
1.69	15.50 ± 0.97	0.5	326.7	327.7	−3238 ± 665		9.56 ± 1.99

[a] The fourth row shows the best-fit parameter values for fitting the experimental data to eq 2. [b] The value for the exponent ν needed to be fixed in the fitting procedure in order to obtain reasonably small errors for the other fit parameters. The value of 1/2 is sensible (see the text). [c] The error of T_c is smaller than 1.5×10^{-2} K.

phenomena may be of the same complex origin, which we briefly sketched in (iii) and which is further discussed in ref 1.

Salt Effects on the Pitch. The pitch−temperature behavior for all chiral samples is shown in Figure 4a.

The solid lines represent the results of the fitting procedure, which we will discuss and analyze later according to the considerations in the Theoretical Basis section. The effects of CsCl on the phase behavior, discussed in the previous section, are directly visible in Figure 4a. Especially pronounced is the shift of the $P(T)$ curves to higher temperatures with increasing CsCl content. Note that for each sample, the end point of the fit curve represents the entry of the two-phase region with the isotropic phase. (The low-temperature border to the chiral nematic phase, $T(L_\alpha{}^*N^*)$, is given in Table 1.) Also, the slight broadening of the N* phase at moderate CsCl concentrations and the narrowing of the N* phase at higher salt content is visible from the figure.

For the determination of the salt effect on the pitch, the authors of previous investigations, Goozner et al. and Ocak et al., compared the pitch of samples with different salt content at a constant temperature. In our case, this is not feasible since there is no temperature at which all samples are in the chiral nematic state; see Figure 4a. The salt-induced shift of the phase boundaries is so strong that the samples with lower CsCl content are isotropic at temperatures below $T(L_\alpha{}^*N^*)$ for the salt-rich samples. Besides this practical problem, we have demonstrated in the Introduction (see Figure 2) that the method of analysis chosen by Goozner and Ocak may result in an apparent salt effect since this method neglects two relevant temperature-dependent phenomena, (i) the temperature dependence of the pitch and (ii) the salt effect on the thermal stability of the N* phase. Using the method of direct pitch comparison at constant temperature on our experimental data, at temperatures where this is possible, yields likewise an apparent salt effect. The N*

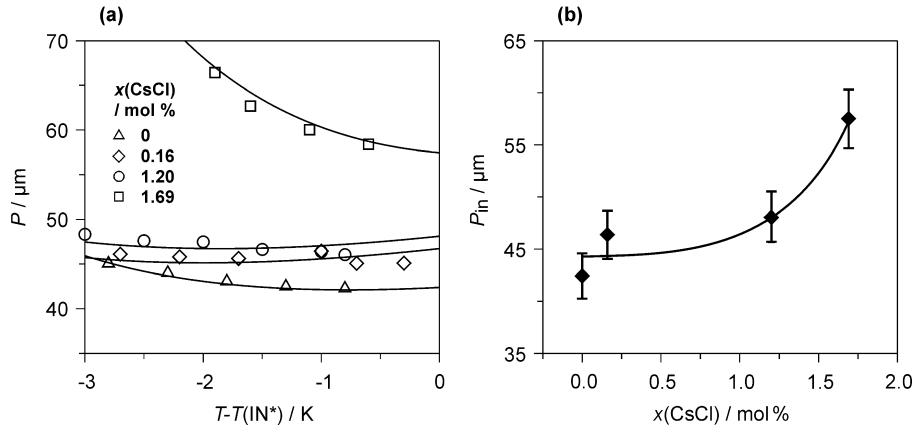

Figure 5. (a) Extract from the pitch−temperature behavior for different CsCl concentrations plotted versus the relative temperature $T - T$(IN*). The solid lines are the best fits of eq 13 (see Table 1 and the text for details). (b) Initial pitch P_{in} at T(N*I) derived from the curves in (a) as a function of the CsCl concentration. The experimental error of the pitch is given. The solid line is a guide to the eye.

phases of the samples with 1.20 and 1.69 mol % CsCl coexist between 55 and 58 °C. The pitch difference at 55 °C is as large as 88 μm and decreases with increasing temperature down to about 10 μm. The difference between the extreme values should be considered as the apparent salt effect since it arises in first order only from the interplay of phenomena (i) and (ii).

In order to reveal the real salt effect on the pitch, the phenomena (i) and (ii) have to be eliminated. For the temperature dependence of the pitch, this is, of course, hard to achieve, but the salt-induced shift of the phase boundaries can be eliminated easily by choosing a temperature relative to any of the transition temperatures. In Figure 4b and c, the $P(T)$ curves are presented with respect to both relative temperatures $T - T$(N*L$_\alpha$*) and $T - T$(N*I), respectively. The similar shape of the $P(T)$ curves with different salt content is striking. All of the $P(T)$ curves show the same course and even partial overlap. This is evidence that the pitch−temperature behavior and also the pitch itself remain, in first order, unaffected by the added salt.

However, with increasing CsCl content, the $P(T)$ curves are slightly shifted to higher pitch values. This offset becomes visible in Figure 4c as the difference of the initial pitch values (P_{in}) far away from the transition into the lamellar phase. As the initial pitch, we chose the pitch value at T(N*I) because in the sample with 1.69 mol of CsCl, the smectic fluctuations appear already close to T(N*I). Since a direct measurement of the pitch at T(N*I) is not feasible, we derived the approximate P_{in} values from the $P(T)$ fit curves (see Figure 5a).

At low CsCl concentrations, the initial pitch appears to be approximately salt-independent (within the experimental error), but P_{in} increases substantially for the sample with the highest CsCl content (see Figure 5b). This means that the high salt concentrations inhibit the twist of the director field.

As the origin of this phenomenon, several mechanisms can be discussed. From the analysis of the salt effects on the phase behavior, we know that the added salt changes both the micellar size and anisotropy. This could, in principle, influence the elastic constants and, thereby, the pitch. Furthermore, added salt could change the charge distribution at the micellar surface and, thereby, screen dispersive chiral interactions. Another aspect that is potentially influenced by added salt is the dopant dynamics, which has been found recently to be important for the chiral induction in another chiral LLC system.[11] However, a clarification of these hypotheses will require further studies.

An interesting hint for the origin of the small salt effect on the pitch is provided by investigations on the salt influence on the solubilization of amphiphilic solutes in aggregates of ionic amphiphiles. Salt was found to hinder the solubilization via screening of the ionic head groups at the micellar surface.[26] Transferred to our case, this means that the effective concentration of D-Leu in the micelle decreases with increasing salt concentration. This, indeed, could account for a reduced helical twist, provided that the chiral induction from the chiral solute onto the phase depends on the direct solute−surfactant interaction in the micelle. Detailed models and mechanisms of the various steps of chirality transfer from the atomic to the macroscopic level have been described and investigated by Kuball et al.[27] One step, in fact, is the direct transfer from the dopant to the surfactant molecule. In light of these considerations, the salt effect on the pitch could be understood as evidence for the correlation of the dopant solubilization in the micelle with its chiral induction. This correlation, in turn, suggests that the steric interaction between the dopant and amphiphile is the important chiral induction mechanism in our system. This result is consistent with the analysis of the salt effect on the pitch−temperature behavior given in the next section.

Pitch−Temperature Behavior and Effects of Salt. As described in the Introduction and derived in the Theoretical Basis section, the shape of the pitch−temperature curve provides information on the chiral induction mechanism in a given dopant−host phase system. The analysis of the $P(T)$ behavior can be carried out by using different model functions to fit the experimental data. For our system, we analyze the $P(T)$ curve exemplarily for the sample with 1.20 mol % CsCl, while the result of this fitting analysis is also valid for all other samples.

Figure 6 shows the experimental $P(T)$ curve for the sample with 1.20 mol % CsCl (open circles).

The curve has pronounced hyperbolic character, and the pitch increases strongly close to the transition into the lamellar phase. This behavior is known from many thermotropic N*−SmA* transitions and originates from the formation of small smectic clusters (cybotactic groups) of a certain coherence length close to the transition.[14,15] As described in the Theoretical Basis section, the function $P(T)$ close to the transition is approximately given by eq 2

$$P = P_0 + \kappa(T/T_c - 1)^{-\nu} \quad (2)$$

where T_c is the apparent critical temperature which lies below the transition temperature in the case of the first-order transition.

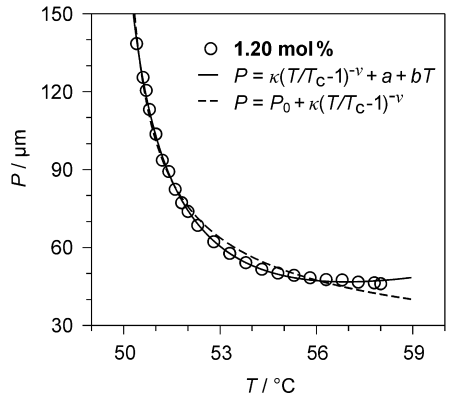

Figure 6. Experimental pitch−temperature behavior for the sample with 1.20 mol % CsCl (open circles) and the best fit by eqs 2 (dashed line) and 13 (solid line). The best-fit parameter values are given in Table 1.

The occurrence of a hyperbolic $P(T)$ function over the whole chiral nematic temperature regime of a lyotropic system indicates that the chiral induction is dominated by chiral steric interaction, that is, by the induction mechanism (B) described in the Introduction and eq 11 in the Theoretical Basis section. The dashed line in Figure 6 is the best fit of eq 2 to the experimental data. The critical exponent ν in thermotropic cases is found to be typically between 0.5 and 0.7.[3,4] Theoretically, a value of 2/3 is expected in case the system behaves like fluid helium, but also, a value of 1/2 can be deduced.[14] In our fitting procedure, we have chosen and fixed the value of 1/2 in order to obtain reasonably small errors for the other fit parameters. (The choice of values like 1/3 or 2/3 gave equally good fitting results, and the fit parameters varied only slightly.) The fit parameters are given in Table 1.

Equation 2 does not follow the experimental curve accurately, even in the vicinity of the lamellar phase. In the high-temperature regime, close to the transition into the isotropic phase, the experimental behavior has clearly more the character of a linear increasing function than that of a hyperbola. A linear contribution to the $P(T)$ behavior is discussed in the Theoretical Basis section for temperatures far away from $T(\mathrm{N^*L_\alpha^*})$ (see eqs 11 and 12 in the Theoretical Basis section). The equation valid for the whole temperature interval of the N* phase is given by eq 13, as described in detail in the Theoretical Basis section.

The solid line in Figure 6 represents the best fit of eq 13 to the experimental data for $\nu = 1/2$, which was chosen as discussed above. The other fit parameters are given in Table 1. In fact, eq 13 describes the experimental data very accurately both in the high-temperature region and close to $T(\mathrm{N^*L_\alpha^*})$. The linear contribution to the pitch−temperature behavior due to the chiral dispersion interaction is clearly important in our system. This is evidence that in the present LLC system, both dispersive and steric chiral induction mechanisms play a significant role.

Information about the proportion of both induction mechanisms can be gained from a detailed analysis of the fit parameters a and b since these depend on the chiral coefficients λ_{att} and λ_s. A first observation is that coefficient a is negative while b is positive. Given the fact that the coefficients λ_{att} and λ_s generally possess opposite signs because they are determined by intermolecular attraction and repulsion, respectively, the positive sign of the coefficient b can only be obtained if $\lambda_s < 0$ (and $\lambda_{att} > 0$) as the contributions to the elastic constants are supposed to be positive. In this case, the negative sign of the coefficient a can be achieved readily if $\lambda_{att} < |\lambda_s k_B T|$ is valid, that is, if the steric repulsion makes a larger contribution to the total helical twisting power. Thus, the experimental data indicate that the steric chiral interaction is more important at all salt concentrations in this system.

The salt effect on the fit parameters a and b is given in Figure 7a. The absolute values of both fit parameters show a very similar nonlinear increase upon the addition of CsCl. The origin of this behavior may be complex since both fit parameters depend on several variables. However, we assume that the elastic constants remain approximately unchanged by added salt and that the first term in the equation for parameter a (see eq 13) dominates its value. Then, the absolute value of the parameter a is increased only if the denominator of the term $(K_{att} + K_s k_B T_0)/(\lambda_{att} + \lambda_s k_B T_0)$ is decreased. This can be achieved, in principle, either by increasing λ_{att} or decreasing the absolute value of λ_s, given from the discussion above that λ_s has to be negative while λ_{att} is positive but smaller than the absolute value of the term $\lambda_s k_B T$. Here, we have to distinguish because only one possibility is meaningful. We know from the previous section that salt increases the pitch; hence, according to $P = K_{22}/\lambda$, added salt should decrease and not increase the chiral coefficient. In this way, we conclude that the added salt decreases the absolute value of λ_s. In other words, salt appears to inhibit the chiral steric interaction.

An interesting result from the fitting procedure is the order of the N*−$\mathrm{L_\alpha^*}$ phase transition in the present case. All fitted T_c values are smaller than the measured $T(\mathrm{N^*L_\alpha^*})$ values, which indicates that the transition is of the first order for all investigated

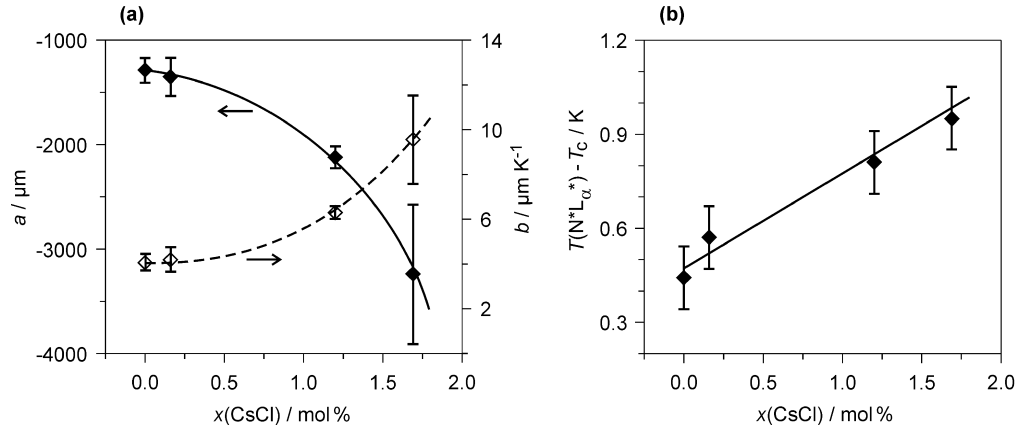

Figure 7. Salt dependence of (a) the fit parameters a and b and of (b) $T(\mathrm{N^*L_\alpha^*}) - T_c$. Note the different scaling for a and b in (a). The curves are guides to the eye.

samples. It is interesting to note that the difference $T(N^*L_\alpha^*) - T_c$ increases approximately linearly with increasing CsCl concentration, as shown in Figure 7b. The same observation has been reported for the isotropic−nematic transition of a slightly more diluted CsPFO/water sample upon the addition of CsCl.[28] In the latter case, the isotropic−nematic transition is only very weakly first order for the salt free sample, and the effect is much stronger since it reaches more than 1 order of magnitude at about 1.7 mol % added salt. However, a clear explanation for this is not given.

Summary and Conclusion

In this paper, we investigated the effect of added CsCl on the absolute value and temperature variation of the helical pitch P of a chiral nematic host phase composed of the surfactant cesium perfluorooctanoate, water and the chiral dopant D-Leucine. The salt effect on the phase boundaries has also been studied. The most pronounced effect of adding electrolytes to a chiral nematic LLC phase corresponds to the phase behavior. The latter is affected in the same way as known for nonchiral LLC systems, that is, the LLC phase transition temperatures are substantially elevated. In contrast, the pitch and the pitch−temperature behavior of the chiral nematic phase are, in the first approximation, not affected by the added salt, provided that the salt effect on the phase behavior is accounted for. In other words, the temperature variation of the pitch is only weakly affected by the salt concentration, provided the pitch is considered as a function of the relative temperature counted from the temperature of the nematic−lamellar transition. In this system, the salt effect is mainly reduced to a substantial change in the transition temperatures between different phases, while the temperature dependence of the pitch inside of the chiral nematic phase remains qualitatively the same. As a result, one may observe a strong apparent salt effect on the value of the helical pitch measured at the same absolute temperature for different mixtures, which is mainly determined by the salt-induced shift of the phase boundaries and not by a direct effect of salt concentration on the chiral induction mechanism.

At high salt concentration, the pitch is slightly increased, which indicates a weak salt-induced inhibition of the chiral induction. The origin of this effect can potentially reveal new aspects of the chiral induction mechanism. Therefore, it is discussed in the context of the existing knowledge, taking into consideration the salt effect on the solubility of chiral dopants within the micelles. This discussion results in evidence that steric chiral interactions are important for the chiral induction in the present case which is consistent with the analysis of the results using our theoretical consideration.

As shown in the theoretical part, the helical pitch in the chiral nematic lyotropic phase is approximately determined by two main contributions. The first contribution stems from pretransitional critical fluctuations, which result in a strong increase of the pitch when approaching the chiral nematic−lamellar transition temperature. This effect is well-known in thermotropic chiral nematics. The second contribution, which is specific for lyotropic systems, is characterized by a linear or hyperbolic temperature dependence and is important far away from the transition into the lamellar phase.

The parameters of the theoretical expression for the pitch have been determined by fitting the experimental data. The analyses of the signs and salt concentration dependence of these parameters reveal the importance of both dispersion and steric chiral interactions and the dominant role of steric chiral interactions in the chiral induction mechanism in the present case. In conclusion, studying the salt effect on the pitch and its temperature behavior is a promising tool toward a better understanding of the chiral induction in LLCs from ionic surfactants. However, care has to be taken in separating the multifaceted salt effects in a LLC system, and future experimental and theoretical studies will be needed in order to complete the present picture of the complex chiral induction mechanisms in LLCs.

Acknowledgment. We thank Cyril Gosselin for support with the measurements. We also acknowledge the financial support from the DFG (Deutsche Forschungsgemeinschaft).

References and Notes

(1) Dawin, U.; Lagerwall, J. P. F.; Giesselmann, F. *J. Phys. Chem. B* **2009**, *113*, 11414–11420.
(2) (a) Baessler, H.; Labes, M. M. *J. Chem. Phys.* **1970**, *52*, 631–637. (b) Stegemeyer, H. *Ber. Bunsen-Ges. Phys. Chem.* **1974**, *78*, 860869;(c) Finkelmann, H.; Stegemeyer, H. *Ber. Bunsen-Ges. Phys. Chem.* **1978**, *82*, 1302–1308.
(3) Pindak, R. S.; Huang, C. C.; Ho, J. T. *Phys. Rev. Lett.* **1974**, *32*, 43–46.
(4) Chen, S. H.; Wu, J. J. *Mol. Cryst. Liq. Cryst.* **1982**, *87*, 197–209.
(5) Dequidt, A.; Oswald, P. *Eur. Phys. J. E* **2006**, *19*, 489–500.
(6) Hiltrop, K. Phase chirality of micellar lyotropic liquid crystals. In *Chirality in Liquid Crystals*; Kitzerow, H.-S., Bahr, C., Eds.; Springer: Berlin, Germany, 2001.
(7) Partyka, J.; Hiltrop, K. *Liq. Cryst.* **1996**, *20*, 611–618.
(8) Pape, M.; Hiltrop, K. *Mol. Cryst. Liq. Cryst. Sci. Technol., Sect. A* **1997**, *307*, 155–173.
(9) Radley, K.; Saupe, A. *Mol. Phys.* **1978**, *35*, 1405–1412.
(10) Osipov, M. A. *Nuovo Cimento D* **1988**, *10*, 1249–1262.
(11) (a) Dawin, U. C.; Dilger, H.; Roduner, E.; Scheuermann, R.; Stoykov, A.; Giesselmann, F. *Angew. Chem.* **2010**, *122*, 2477–2480. (b) Osipov, M. A.; Dilger, H.; Roduner, E.; Scheuermann, R.; Stoykov, A.; Giesselmann, F. *Angew. Chem., Int. Ed.* **2010**, *49*, 2427–2430.
(12) Goozner, R. E.; Labes, M. M. *Mol. Cryst. Liq. Cryst.* **1985**, *116*, 309–317.
(13) Ocak, Ç.; Acımı, M.; Akpınar, E.; Gök, A. *Phys. Chem. Chem. Phys.* **2000**, *2*, 5703–5707.
(14) de Gennes, P. G. *The Physics of Liquid Crystals*; Clarendon Press: Oxford, U.K., 1979; p 321.
(15) de Gennes, P. G.; Prost, J. *The Physics of Liquid Crystals*; Clarendon Press: Oxford, U.K., 1998; pp 514−518.
(16) Osipov, M. A. Molecular Theories of Liquid Crystals. In *Handbook of Liquid Crystals*; Demus, D., Goodby, J. W., Gray, G. W., Spiess, H.-W., Vill, V., Eds.; Wiley-VCH: Weinheim, Germany, 1998; Vol. 1.
(17) Osipov, M. A. Molecular Theory of Cholesteric Polymers. In *Liquid Crystalline and Mesomorphic Polymers*; Shibaev, V. P., Lam, L., Eds.; Springer: Berlin & Heidelberg, Germany, 1994.
(18) Wensink, H. H.; Jackson, G. *J. Chem. Phys.* **2009**, *130*, 234911.
(19) Kimura, H.; Hosino, M.; Nakano, H. *J. Phys. Soc. Jpn.* **1982**, *51*, 1584–1590.
(20) van der Meer, B. W.; Vertogen, G. A molecular model for the cholesteric mesophase. In *Molecular Physics of Liquid Crystals*; Luckhurst, G. R., Gray, G. W., Eds.; Academic Press: New York, 1979.
(21) Osipov, M. A.; Kuball, H. G. *Eur. Phys. J. E* **2001**, *5*, 589–598.
(22) (a) Abramoff, M. D.; Magelhaes, P. J.; Ram, S. J. *Biophotonics Int.* **2004**, *11*, 36. (b) Rasband, W. S. *ImageJ*; U. S. National Institutes of Health: Bethesda, MD, 1997−2009; found at http://rsb.info.nih.gov/ij/.
(23) Boden, N.; Harding, R.; Gelbart, W. M.; Jolley, K. W.; Heerdegen, A. P.; Parbhu, A. N. *J. Chem. Phys.* **1995**, *103*, 5712–5719.
(24) Israelachvili, J. N. *Intermolecular and Surface Forces*;, Academic Press: New York, 1991.
(25) Hardy, P. M. The Protein Amino Acids. In *Chemistry and Biochemistry of the Amino Acids*; Barrett, G. C., Ed.; Chapman and Hall: London, 1985; p 9.
(26) Christian, S. D.; Scamehorn, J. F. *Solubilization in Surfactant Aggregates*; Marcel Dekker, Taylor & Francis Group: New York, 1995; p 9.
(27) Kuball, H. G.; Höfer, T. From a chiral molecule to a chiral anisotropic phase. In *Chirality in Liquid Crystals*; Kitzerow, H.-S., Bahr, C., Eds.; Springer: Berlin, Germany, 2001.
(28) Rosenblatt, C.; Zolty, N. *J. Phys. Lett.* **1985**, *46*, 1191–1197.

JP102547P